AWARD NUMBER: W81XWH-15-1-0074

TITLE: Torsion-Induced Traumatic Optic Neuropathy (TITON): Animal Model for Diagnostics, Drugs Delivery, and Therapeutics for Injuries to the Cental Nervous System

PRINCIPAL INVESTIGATOR: Matthew A. Reilly

CONTRACTING ORGANIZATION: University of Texas at San Antonio
San Antonio, TX 78249

REPORT DATE: June 2016

TYPE OF REPORT: Annual

PREPARED FOR: U.S. Army Medical Research and Materiel Command
Fort Detrick, Maryland 21702-5012

REPORT DOCUMENTATION PAGE

Form Approved
OMB No. 0704-0188

1. REPORT DATE	2. REPORT TYPE	3. DATES COVERED
June 2016	Annual	22 May 2015 – 21 May 2016

4. TITLE AND SUBTITLE

Torsion-Induced Traumatic Optic Neuropathy (TITON): Animal Model for Diagnostics, Drugs Delivery, and Therapeutics for Injuries to the Cental Nervous System

5a. CONTRACT NUMBER

5b. GRANT NUMBER
W81XWH-15-1-0074

5c. PROGRAM ELEMENT NUMBER

6. AUTHOR(S)

Matthew Reilly, Lora Watts, Randolph Glickman, Katelyn Swindle-Reilly, Rena Bizios

E-Mail: reilly.196@osu.edu

5d. PROJECT NUMBER

5e. TASK NUMBER

5f. WORK UNIT NUMBER

7. PERFORMING ORGANIZATION NAME(S) AND ADDRESS(ES)

University of Texas at San Antonio
One UTSA Circle
San Antonio, TX 78249

University of Texas Health Science Center – San Antonio
7703 Floyd Curl Dr
San Antonio, TX 78229

8. PERFORMING ORGANIZATION REPORT NUMBER

9. SPONSORING / MONITORING AGENCY NAME(S) AND ADDRESS(ES)

U.S. Army Medical Research and Materiel Command
Fort Detrick, Maryland 21702-5012

10. SPONSOR/MONITOR'S ACRONYM(S)

11. SPONSOR/MONITOR'S REPORT NUMBER(S)

12. DISTRIBUTION / AVAILABILITY STATEMENT

Approved for Public Release; Distribution Unlimited

13. SUPPLEMENTARY NOTES

14. ABSTRACT

Traumatic optic neuropathy (TON) is a common injury following traumatic insult to the head. A novel animal model of TON will be investigated for the purpose of developing diagnostics and treatments for TON. Magnetic resonance imaging techniques were developed to characterize retinal blood flow, axonal transport within the optic nerve, and functional imaging to allow diagnosis of TON. Matrix assisted laser desorption/ionization techniques have been developed to detect spatially resolved mass spectra for the detection of trauma-induced changes in biomarker expression; these biomarkers will both improve our understanding of the basic mechanisms of TON and may be subsequently investigated for serum-based diagnostics. Preliminary development of a hydrogel material for delivering therapeutics to the site of injury was also undertaken. A finite element model of gel volumetric changes about the optic nerve was developed to allow optimization of gel mechanical and swelling properties to mechanically assist the recovery process.

15. SUBJECT TERMS

16. SECURITY CLASSIFICATION OF:			17. LIMITATION OF ABSTRACT	18. NUMBER OF PAGES	19a. NAME OF RESPONSIBLE PERSON
a. REPORT	b. ABSTRACT	c. THIS PAGE			USAMRMC
U Unclassified	U Unclassified	U Unclassified	UU Unclassified		19b. TELEPHONE NUMBER *(include area code)*

Standard Form 298 (Rev. 8-98)
Prescribed by ANSI Std. Z39.18

Table of Contents

Page

1. Introduction

Traumatic optic neuropathy (TON) is a common battlefield injury subsequent to blast exposure or other head injury resulting in blindness. TON is difficult to diagnose and remains untreatable, at least in part due to the lack of a suitable animal model. In Phase I of this study, we will utilize a novel animal model for TON to develop diagnostic criteria using magnetic resonance imaging, biomarker identification, and neurophysiology. In Phase II, candidate therapeutics will be evaluated for efficacy in reversing TON.

2. Keywords

Traumatic optic neuropathy; magnetic resonance imaging; matrix assisted laser desorption/ionization; drug delivery; hydrogel; nerve regeneration

3. Accomplishments

GOAL 1: DEVELOP AND VALIDATE MAGNETIC RESONANCE IMAGING DIAGNOSTICS (5% COMPLETE)

MRI has become a powerful diagnostic tool because it can provide non-invasive anatomical, physiological and functional information in a single setting. Diffusion-weighted imaging (DWI) is an MRI-based technique which image contrast is based on diffusional water motion. Diffusion tensor imaging (DTI) is a multi-directional DWI technique used to estimate apparent diffusion coefficients and fractional anisotropy (FA) as metrics for structural changes in white matter. A DTI sequence was developed for this study to allow quantification of optic nerve structure before and after injury. A perfusion-weighted MRI sequence was developed to quantify localized retinal blood flow.

Retinal Blood Flow: We have implemented the arterial spin-labeling technique with a separate neck labeling coil and snap-shot gradient echo-planar imaging to measure quantitative blood flow in the rat retina. A butterfly neck coil is placed at the position of the common carotid arteries for arterial spin labeling. The neck and the eye coils are actively decoupled. The following parameters will be used: slice thickness = 1 mm, TR = 4 s, TE = 13 ms, label duration = 2.1 s, and 20 repeats each with and without labeling will be acquired for 16 min scans. Quantitative BF images in units of (ml blood)/(g tissue)/min will be calculated using the equation

$$BF = \frac{\lambda}{T1}\frac{SNL - SL}{2\alpha M0\left(1 - e^{-LD/T1}\right)},$$

where SNL and SL are signal intensities of the non-labeled and labeled images, respectively, λ is the water tissue-blood partition coefficient (0.9), and M0 is the equilibrium value of magnetization directed along the direction of the static magnetic field. The retina and choroid T1 at 11.7 T is 2.1 s. The labeling efficiency α is 0.75. Blood flow is relatively constant along the length of the retina as a function of distance from the optic nerve head, except that it drops significantly at the distal edges where the retina terminates. The average whole-retina blood flow is 6.3 ± 1.0 mL/gram/min (mean ± SD, n = 6) under 1.1% isoflurane. These findings are consistent with blood flow in the retina obtained in the same animals using microsphere techniques.

DTI MRI will be acquired with spin-echo EPI with diffusion-sensitizing gradients applied in 32 orthogonal directions with b = 1000 s/mm^2, and one scan with b = 0, slice thickness = 1 mm, TR = 3 s, TE = 35 ms, FOV = 12.8x12.8, matrix = 128x128, in-plane resolution = 100x100 μm, 4 shots, 30 diffusion directions. Quantitative ADC maps in units of mm^2/s and fractional anisotropy (FA) will be calculated from the DTI data.

These experiments will commence immediately after receiving approval from the Animal Care and Use Review Office (ACURO).

GOAL 2: BIOMARKER DISCOVERY AND LOCALIZATION (15% COMPLETE)

Preliminary experiments were conducted using animals previously subjected to unilateral injury stimulus and sacrificed after one week. Eyes were removed with 3-5 mm of optic nerve intact taking care not to stretch or otherwise injure the nerve. Eyes were flash frozen in liquid nitrogen, then stored at -80°C. The eyes were then sectioned through the optic nerve using a cryostat, then transferred to indium titanium oxide-coated slides, which were subsequently coated with a dihydroxybenzoic acid (DHBA) matrix.

We have been practicing tissue preservation, preparation, and MALDI techniques on tissue that was previously taken from another animal study to optimize tissue treatment prior to commencing a new animal study. We have determined that the proteins will be successfully identified with the method originally proposed (Figure 1) and that tissues stored for longer periods of time are not well preserved even at ultracold temperatures (Figure 2). Future experiments will include running a trypsin digest on control eyes and experimental eyes to determine the specific peptides present in the samples, thereby allowing differential analysis to indicate which changes are due to injury.

We will continue to perfect our methods on tissue preparation, specifically the procedure used to embed the tissue for slicing as it has been recently learned that the OCT used is not MALDI compatible and can potentially bleed into the sample. A new technique using a gelatin mold is currently being considered as the best method for tissue embedding. While we hope to see protein changes in the retina and optic nerves of our experiments, our current runs show changes only in the retina as well as some changes inside the eye which could be the lens. It would be notable to see changes in the lens with our future experiments but it is not expected as the lens does not easily stay intact during the slicing process. Further, heat stabilization techniques are also being considered as it allows cross linking of the proteins of interest and stops the process of degradation permanently after the tissue have been taken from the subject. This approach helps the analytical results of the experiment to be as close to the in vivo state as possible and has been proven to be compatible with MALDI imaging.

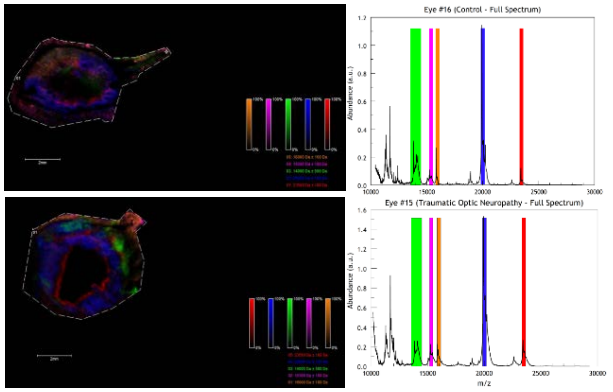

Figure 1: Pseudocolor MALDI spatial analysis from eyes shortly after completion of experiments. Above: Localized protein spectrum from MALDI analysis of a control eye. Below: Localized protein spectrum from MALDI analysis of an eye one week after onset of traumatic optic neuropathy. Left: A pseudocolor mage of the tissue section showing the spatial distributions of the proteins. Right: Protein mass spectrum. The color boxes indicate the m/z values of the color-coded areas in the pseudo-color image above.

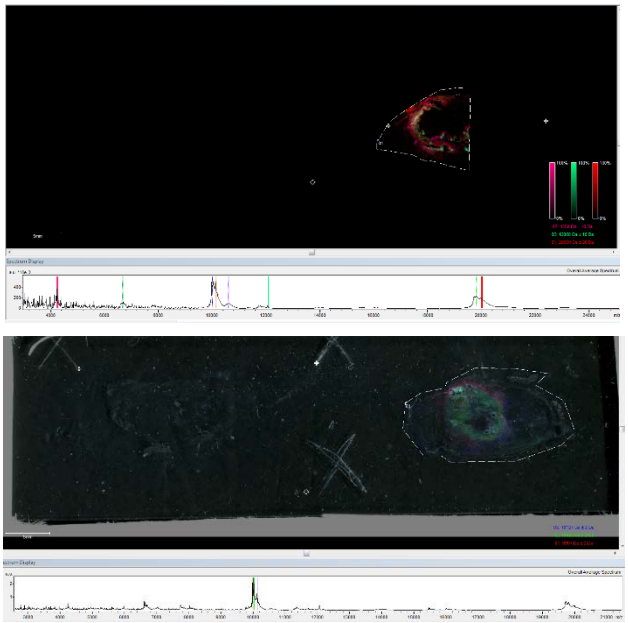

Figure 2: Pseudocolor MALDI spatial analysis from eyes stored at -70°C for six months. Significant degradation of the proteins has occurred, indicating the need for processing and analysis of tissue samples shortly after completion of experiments.

GOAL 3: ESTABLISH IN VITRO NEURONAL INJURY MODEL (0% COMPLETE)

Nothing to report.

GOAL 4: DEVELOP DRUG DELIVERY VEHICLE (15% COMPLETE)

Work has been initiated to develop a novel hydrogel "cast" which will locally deliver neuroprotective agents to the site of TON injury. In addition to testing collagen by itself for the hydrogel system, semi-interpenetrating polymer networks (semi-IPNs) were formed by combining hydrogel-producing polysaccharides with the collagen (protein-based) network. The addition of these polysaccharides to the collagen protein is expected to cause greater hydrogel contraction than collagen by itself because of the innate sol-gel transitions of the polysaccharides, as well as greatly increased hydrogen bonding between protein and polysaccharide. Hydrogel contraction was observed visually for these combinations. Collagen gels were prepared alone and with the addition of several biocompatible polysaccharides including gellan, three varieties of alginate, iota-carrageenan, kappa-carrageenan, xanthan gum, cellulose, carboxymethylcelluose, and pullulan. The most promising candidates were collagen gels alone or in combination with alginate, iota-carrageenan, or gellan gum.

Studies are ongoing to optimize the both the polymer concentration and salt concentration in the gels to obtain the optimal mechanical properties and gel contraction upon formation. The ratios of collagen to polysaccharide are being investigated in addition to the total ratio of polymer to aqueous solution in the gel. Viscoelastic properties of hydrogels will be evaluated using a Malvern rheometer.

Preliminary stability studies were initiated to determine whether mixing collagen with the polysaccharides prior to injection was feasible by blending the polymers and refrigerating the solutions. Blends prepared in distilled water and phosphate buffered saline were stored in the refrigerator. All gelled or phase separated in the refrigerator in less than 24 hours indicating lack of stability in liquid form when premixed. Addition of saline with calcium and magnesium did not cause further gelation indicating there was gel formation followed by collapse. This result indicates that a combination system would potentially need to be co-injected using a dual chamber syringe prior to the procedure. This approach, rather than having a premixed solution available, is commonly employed for similar ocular systems, such as fibrin glue.

Polytetrafluoroethylene (PTFE) molds have been fabricated to allow characterization of sample swelling. These molds were made from high-precision (1/4" thickness) PTFE to ensure accurate initial volume estimation. Through-holes were drilled using a 10 mm-diameter drill bit. Thus, each hole had a volume of 498.7 µL. Two identical PTFE sheets were placed above and below the drilled sheet and rigidly clamped to form a seal. PTFE with a "slippery" finish was chosen because it is very hydrophobic, allowing the samples to be easily removed from the drilled holes after gelation.

A protocol was developed to allow quantification of methylene blue (MB) released by the drug delivery vehicle. MB was diluted between 0.01-10 µg/mL in a mobile phase comprised of 20 mM sodium acetate, 12.5 mM 1-octanesulfonic acid, 38% acetonitrile, and the balance distilled water. The solution was adjusted to pH 3.85 with acetic acid and checked with a pH meter. An ultra-performance liquid chromatography (UPLC) column (BEH C18; Waters Corporation; Milford, MA) was used to separate methylene blue from any impurities while a photodiode array detector was used to measure sample absorption at wavelength 290 nm as a function of retention time within the column. This approach yielded a retention time for methylene blue of about 4 minutes (Figure 3). The lower limit of quantitation (LLOQ) and limit of detection (LOD) were determined to be 0.5 µg/mL and 0.05 µg/mL, respectively (Figure 4).

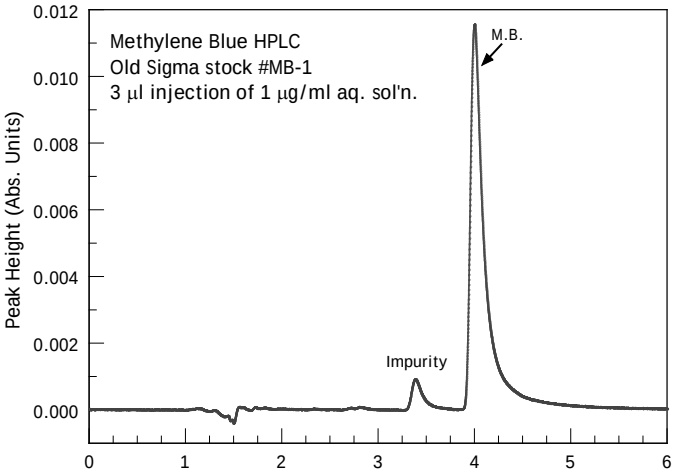

Figure 3: Chromatogram showing methylene blue separation from a 3 µL sample injected at 1 µg/mL.

Increasing the sodium acetate buffer strength from 10 mM to 20 mM and controlling pH to 3.8 gave improved peak shape, although

some peak tailing remains. Increasing buffer strength to 25 mM did not yield further improvement. Because the peaks are somewhat asymmetrical, quantitation by peak area is expected to yield more consistent results. This was in fact the case; the linearity was slightly greater using peak area compared to peak height. In terms of practical quantitation, however, the difference is negligible. The linearity of the analytical results dropped off markedly at dilutions below 0.5 µg/mL, although dilutions down to 0.05 µg/mL were detectable. From these observations, it was concluded that the present method has an LLOQ of 0.5 µg/mL and an LOD of 0.05 µg/mL. Translating this to quantification of MB release during a release experiment (i.e. quantifying absolute amounts of MB release regardless of dilution), this equates to an LLOQ of 150 picograms and an LOD of 15 picograms. This resolution should be sufficient for quantifying MB release in the present study.

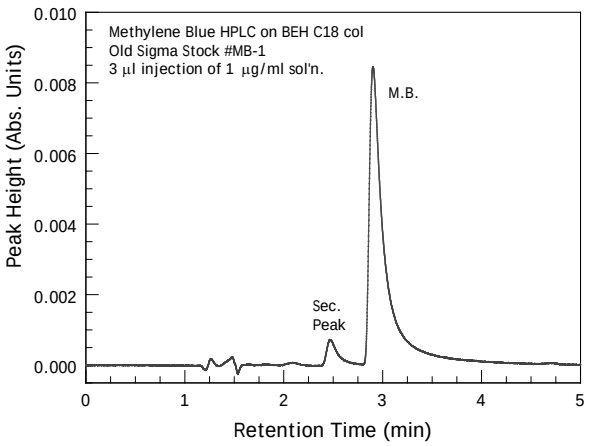

Figure 4. HPLC separation of methylene blue, 1 µg/ml, from the secondary peak, using the modified LC method described in the text. The retention times of the analytes was about 1 min shorter than in the original method.

Analysis of Secondary Peak in Methylene Blue Solutions

As illustrated by the chromatogram shown in Figure 3, in solutions of methylene blue a secondary peak was detected that eluted from the column approximately 30 s before the main compound peak. This secondary peak is labeled as an impurity in Figure 3; however, it was not identified at the time of the original HPLC analysis. Therefore, subsequent work has been carried out to identify this peak. To do so, the LC method has been modified slightly to optimize it for liquid chromatography- mass spectrometry using electrospray ionization (LC-MS-ESI). In order to maximize the volatility of the soluble components of the mobile phase, the ion pair agent was changed from octanesulfonic acid to methanesulfonic acid, while the buffer remained the same. The working mobile phase for the LC-MS-ESI analysis was 20 mM ammonium acetate (pH 5.0), 20 mM methanesulfonic acid, 38% acetonitrile, with the balance distilled H_2O. The analytical column was the BEH C18 used in the initial work, maintained at 30° C. The mobile phase flow rate was 0.1 ml/min. With these modified conditions, the main methylene blue peak was well separated in LC from the secondary peak, with the overall retention times reduced by about 1 min (Figure 4), compared to those obtained in the original method (Figure 3).

This LC method was successfully ported to the mass spectrometer. The analysis was carried out using a Waters Acquity I-class LC unit as the input to a Waters TQD triple quadrupole mass spectrometer. An injection volume of 3 µl of the methylene blue samples was used in all of the analyses, which produced peaks in the total ion chromatograms at the same retention times as in the HPLC analysis. This may be appreciated by comparing the peak retention times in Figure 4 (HPLC) to those in Figure 5 (LC-MS). The peak eluting at 2.96 min has an m/z of 284, which is the expected m/z of the methylene blue molecular ion. The species eluting in the secondary peak at 2.58 min has an m/z of 270. This species can be identified as the N-demethylated derivative of methylene blue, produced by the loss of a CH_2 (= 14 amu) from the parent molecule. Tertiary amines readily undergo such oxidative reactions and have been previously reported for solutions of methylene blue.[1, 2]

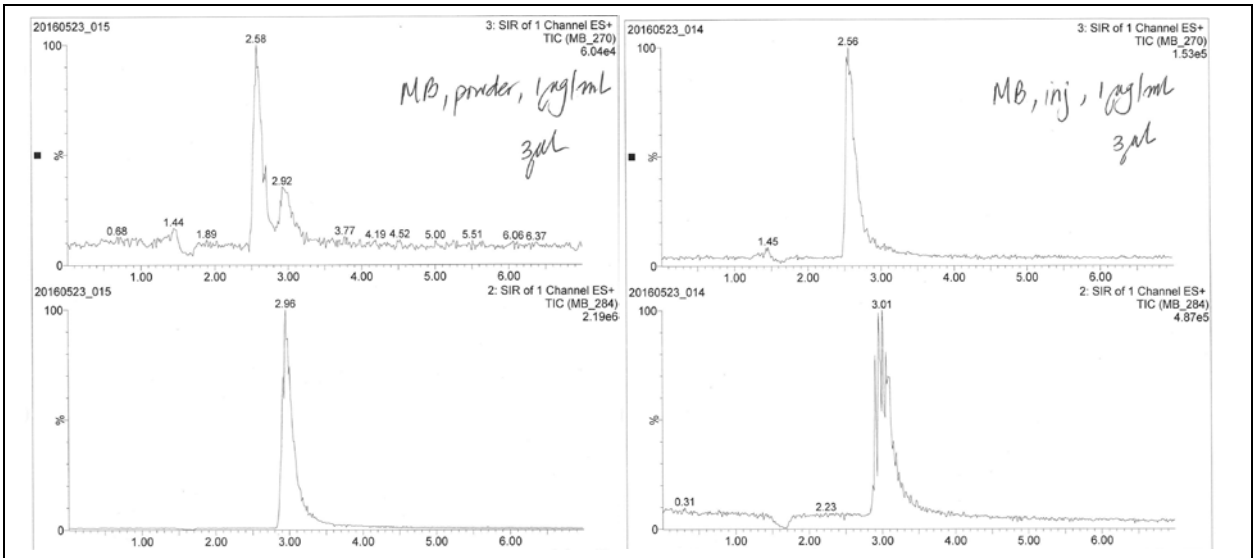

Figure 5. Mass chromatograms of methylene blue (MB) solutions. The upper portion of each panel shows the total ion chromatogram for the m/z 270 species (retention time ~2.56 min), while the lower portion of each panel shows the total ion chromatogram of the m/z 284 species (retention time ~2.7 min). Left panel: injection of 3 µl of a 1 µg/ml solution of MB prepared from dry powder (Sigma MB-1). This solution had aged for about 5 weeks from the time it was originally made until this analysis. Right panel: injection of 3 µl of a 1 µg/ml aliquot of the injectable preparation of MB (Akorn). Note that the peak of this particular compound was noisy, leading to a broader peak.

Both the 270 and 284 peaks were subjected to collision (MS/MS) analysis. The 284 parent ion gave rise to daughter ions at m/z = 268, 254, and 240, corresponding to the loss of a single methane (CH_4), a double methane, and a dimethylamine group, respectively. The 270 parent gave rise to daughter ions at 254, 228, and 226, corresponding to the loss of a single methane, double demethylation, or loss of a dimethylamine, respectively. Thus, all of the major ions observed in the mass spectra can be traced back to the parent methylene blue molecular ion. These observations show that the secondary peak in the methylene blue solutions is an oxidation product of the compound and not an impurity. In a methylene blue solution that is maintained in the presence of air, the oxidative demethylation reaction will proceed at some background rate, producing an increasing amount of the derivative. Support for this mechanism is provided by the analysis of a fresh solution of methylene blue, in which a very low level of the demethylated derivative is present (Figure 6).

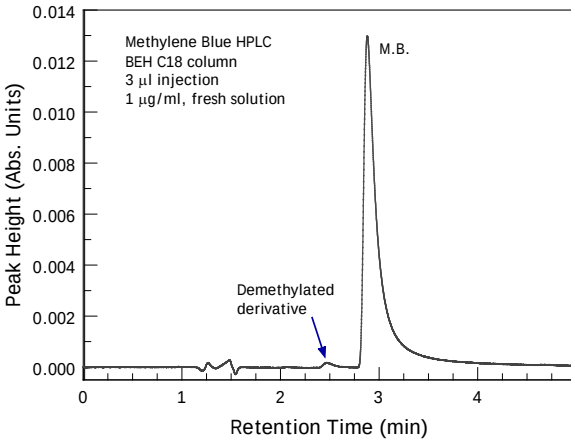

Figure 6. A fresh solution of methylene blue, 1 µg/ml, analyzed by HPLC. The small relative amount of the demethylated derivative in this sample supports the hypothesis that this species is formed by a progressive oxidative reaction in methylene blue solutions.

Data are lacking on the biological activity of the derivative; however, methylene blue is thought to provide neuroprotection by facilitating electron transfer in the nicotinamide adenine dinucleotide system, thereby reducing accumulation of reactive oxygen species. Therefore, the demethylated derivative may still retain some antioxidant activity, albeit reduced, due to several electron acceptor sites remaining on the molecule. In addition, the relative amount of the derivative is small compared to the amount of parent methylene blue present, even in the injectable preparation that has aged for ~1.5 years, and likely represents a negligible change in the overall pharmaceutical activity.

Mechanical Model of Cast Contraction

A finite element model of the hydrogel cast interacting with the optic nerve was developed in COMSOL Multiphysics 5.2 (COMSOL, Inc.; Burlington, MA) to give insight into their mechanical interaction. Briefly, an axisymmetric model describing 3 mm of the optic nerve length was encased by a 1 mm hydrogel cast. The entire optic nerve was modeled as a linear, elastic, homogeneous, isotropic (LEHI) material, as was the cast. Homogeneous displacements were prescribed to all boundaries of the cast to mimic a uniform volumetric contraction while both ends of the nerve were held fixed. A uniform triangular mesh containing 4,132 elements was generated. The resulting strain fields within the nerve were then estimated (Figure 5).

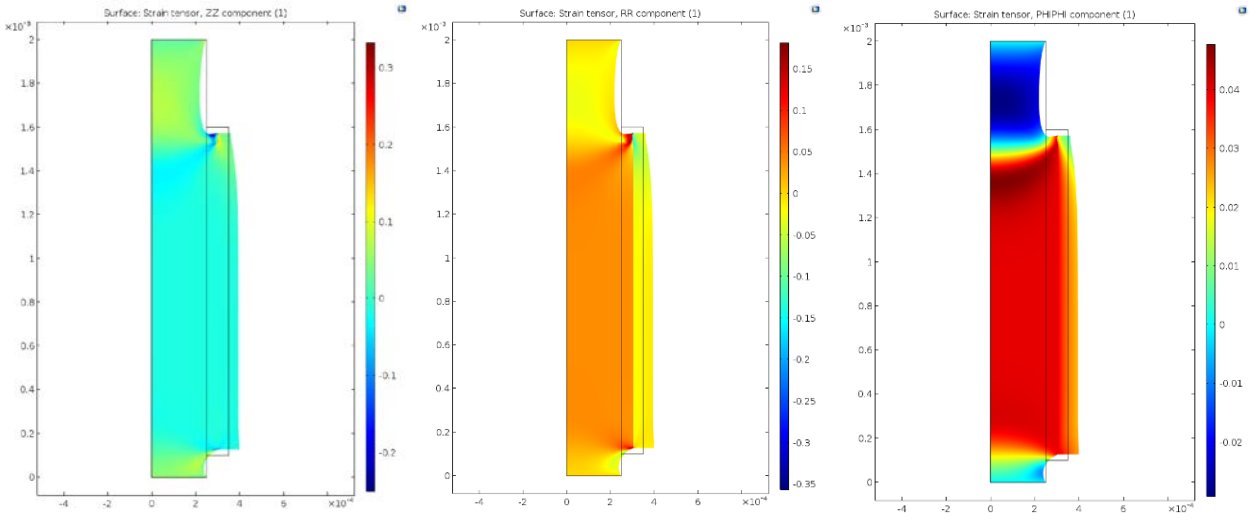

Figure 5: Strain distributions within the optic nerve following a 4% contraction of the cast. The solid line indicates the undeformed geometry while the colored maps indicate directional strains in the deformed configuration following hydrogel contraction. In particular, note that the axial strain (left) is slightly positive outside the casted region and slightly negative within this region. This result implies that the portion of the axons beyond the casted region would be under tension while the portion within the injured region would be under compression. This is the operating principle of the hydrogel cast, which is designed to force the injured ends of axons together within the casted region while maintaining tension on the uninjured portions of the axons. While this model is based on an oversimplification of the optic nerve, it is a first approximation of the expected mechanical performance of the cast system.

GOAL 5: CHARACTERIZE OPTIC NERVE RESCUE BY VARIOUS TREATMENTS (0% COMPLETE)

Nothing to report.

GOAL 6: CHARACTERIZE NEURONAL RESPONSE TO VARIOUS TREATMENTS (0% COMPLETE)

Nothing to report.

4. Impact

Nothing to report.

5. Changes/Problems

We petitioned USAMRMC to transfer the award from the University of Texas at San Antonio to The Ohio State University subsequent to a change of institution by the PI and one co-PI. This development has significantly delayed several aspects of the project, especially the commencement of animal studies. These studies will commence immediately upon approval of award transfer. Expenditures are behind schedule as a result. Animal protocols have been moved from UTSA to UTHSCSA, though the scope of work and experiments will proceed according to the original statement of work.

6. Products

Two abstracts have been presented at international meetings:

- Swindle-Reilly, K.E., Asemota, B.I., Rodriguez, L., Jones, K.R., Glickman, R.D., Reilly, M.A., Development of Animal Model and Hydrogel Delivery System to Treat Traumatic Optic Neuropathy. *Translational to Clinical (T2C) Regenerative Medicine Wound Care Conference*, March 2016.
- Jones, K., Glickman, R.D., Reilly, MA, Torsional Indirect Traumatic Optic Neuropathy (TITON): Identifying Biomarkers of Trauma using Matrix Assisted Laser Desorption/Ionization (MALDI), *Association for Research in Vision and Ophthalmology*, May 2016.

7. Participants & Other Collaborating Organizations

Name:	Matthew Reilly
Project Role:	PD/PI
Researcher Identifier (e.g., ORCID ID):	0000-0001-8029-0084
Nearest person month worked:	1
Contribution to Project:	PI/PD; report preparation; submitted grant transfer information

Name:	Rena Bizios
Project Role:	Co-PI
Researcher Identifier (e.g., ORCID ID):	N/A
Nearest person month worked:	0
Contribution to Project:	Development of in vitro neuronal injury model

Name:	Lora Watts
Project Role:	Co-PI
Researcher Identifier (e.g., ORCID ID):	0000-0002-2337-1504
Nearest person month worked:	0
Contribution to Project:	Development of MRI sequences; Revision of IACUC and ACURO documents

Name:	Randolph Glickman

Project Role:	Co-PI
Researcher Identifier (e.g., ORCID ID):	N/A
Nearest person month worked:	1
Contribution to Project:	Development of MALDI and methylene blue detection techniques

Name:	Kirstin Jones
Project Role:	Graduate Research Assistant
Researcher Identifier (e.g., ORCID ID):	N/A
Nearest person month worked:	3
Contribution to Project:	Development of tissue preparation and MALDI imaging protocols

Name:	Katelyn Swindle-Reilly
Project Role:	Co-PI
Researcher Identifier (e.g., ORCID ID):	N/A
Nearest person month worked:	1
Contribution to Project:	Development of hydrogel “cast” biomaterial

8. Special Reporting Requirements

None

9. Appendices

None

References

1. Van Berkel GJ, Sanchez AD, Quirke JM. Thin-layer chromatography and electrospray mass spectrometry coupled using a surface sampling probe. *Anal Chem* 2002;74:6216-6223.
2. Small JM, Hintelmann H. Methylene blue derivatization then LC-MS analysis for measurement of trace levels of sulfide in aquatic samples. *Anal Bioanal Chem* 2007;387:2881-2886.

Torsional Indirect Traumatic Neuropathy (TITON): Animal Model for Diagnostics, Drug Delivery, and Therapeutics for Central Nervous System Injury

MR130235
W81XWH-15-1-0074

PI: Matthew A. Reilly **Org:** University of Texas at San Antonio **Award Amount:** $1,000,000

Study Aims

- Diagnostics
  - Quantify TITON-induced changes in DTI and MRI
  - Develop serum assays, MALDI-TOF proteomics
- Drug discovery and dosing
  - Develop drug reservoir hydrogel "cast"
  - In vitro dosing assays
  - In vitro drug elution kinetics
- In vivo evaluation of candidate treatments

Approach

We have developed a new physiological model of indirect traumatic optic neuropathy (TON). This non-invasive technique achieves injury relevant to blast by rapidly rotating the eye to localize injury near the posterior insertion of the optic nerve. This model offers a simple platform for evaluating diagnostic and therapeutic modalities for TON. We will evaluate new local approaches to treatment including a novel hydrogel "cast" which also serves as a drug delivery reservoir.

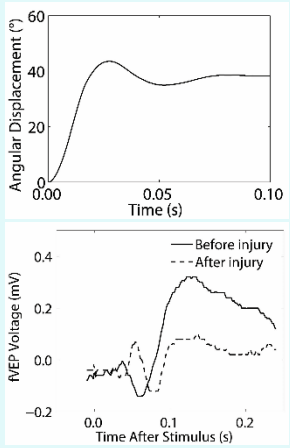

Accomplishment: We have developed a robot which reproducibly applies torsional indirect traumatic optic neuropathy (TITON) in a rat model (left) on the same time scale as an IED blast insult (top right). Flash vision evoked potentials (fVEP) have thus far been used to quantify changes in the visual pathway (bottom right).

Timeline and Cost

Activities CY	Lead	15	16	17	18
Diagnostic imaging validation	Watts				
MALDI biomarker identification	Glickman				
Establish in vitro RGC model	Bizios				
Hydrogel cast for drug delivery	Swindle-Reilly				
Optic nerve rescue in vivo	Reilly				
In vitro europrotective study	Bizios				
Estimated Budget ($K)		**$425**	**$328**	**$137**	**$110**

Updated: 21 June 2016

Goals/Milestones

CY15 Goals – Development of novel materials and methods
☑ Develop MRI, DTI, BF protocols
☑ Optimize MALDI proteomic methodology
☑ Formulate hydrogel cast candidates

CY16 Goal – Validate diagnostics and drug delivery vehicles
☐ Validate imaging (MRI, DTI, BF) protocols in unilaterally injured rats
☐ Quantify changes in protein expression using MALDI proteomics
☐ Characterize and manufacture hydrogel cast/drug delivery reservoir
☐ Develop in vitro RGC injury model

CY17 Goal – Treatment studies
☐ Determine metrics of TON in the in vitro RGC model
☐ Begin in vivo treatment studies in bilaterally injured rats
☐ Characterize treatment efficacy using MRI, DTI, BF

CY18 Goal – Treatment studies
☐ Complete in vitro treatment studies
☐ Complete in vivo treatment studies